Graduate Laboratory **Experiment Nr. 52**

Heavy Ion Scattering at the Tandem Accelerator

M. Weber, C. Herlitzius

April 12, 2010 .

Contents

1 The basics of scattering experiments **3**
1.1 Scattering kinematics 3
1.2 Rutherford scattering 5
1.3 Mott scattering of identical particles 9
1.4 Energy loss in matter 11

2 The Munich Tandem Accelerator **13**
2.1 Overview 13
2.2 Operating Principle of the Tandem Accelerator 13
2.3 Facilities in the Munich accelerator lab 15

3 Safety Instructions **17**
3.1 Potential hazards in the laboratory 17
3.2 Basics of radiation safety 17

4 Experiment setup and execution **19**
4.1 Assembly 19
4.2 Particle detectors 20
4.3 Analog und Digital Signal Processing 24
4.4 Experimental procedure 25

1 The basics of scattering experiments

1.1 Scattering kinematics

Choosing a general ansatz for elastic scattering we assume momentum and energy conservation.

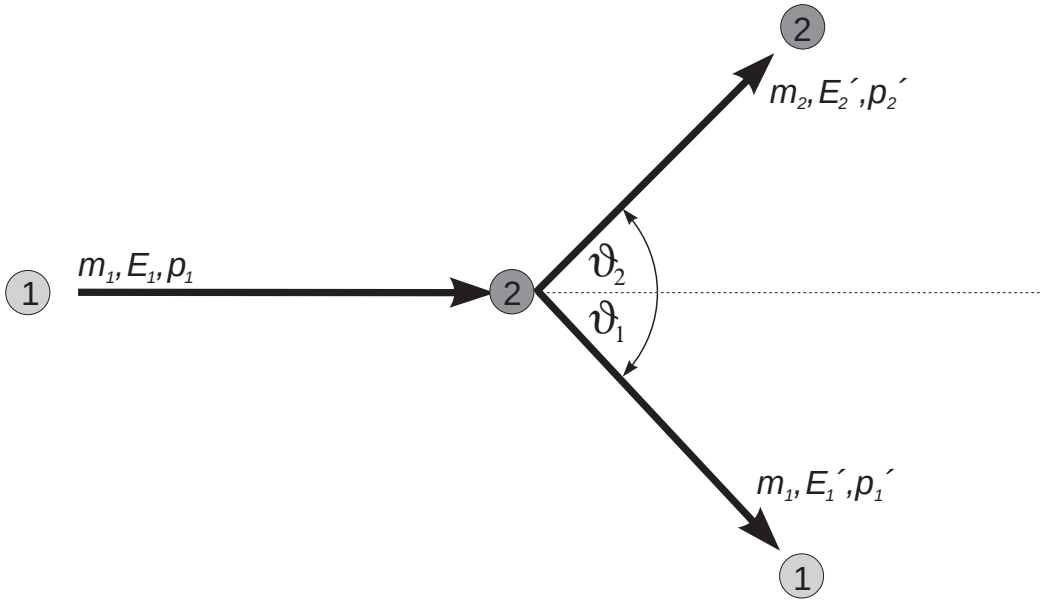

Figure 1: The two body problem with the target at rest

$$\vec{p}_1 + \vec{p}_2 = \vec{p}_1{}' + \vec{p}_2{}' \quad (1)$$

$$E_1 + E_2 = E_1' + E_2' \quad (2)$$

$$(3)$$

The problem becomes even easier to tackle in the Center of Mass System (CMS). There all four momentum vectors involved in the scattering process of two particles are of equal length. (see Figure 2). In the CMS we find for the momentum transfer:

$$\Delta\, p = m_1 \mid \vec{v}_{1CM} - \vec{v}'_{1CM} \mid = 2\, m v_{1CM} \sin\frac{\theta}{2} \quad (4)$$

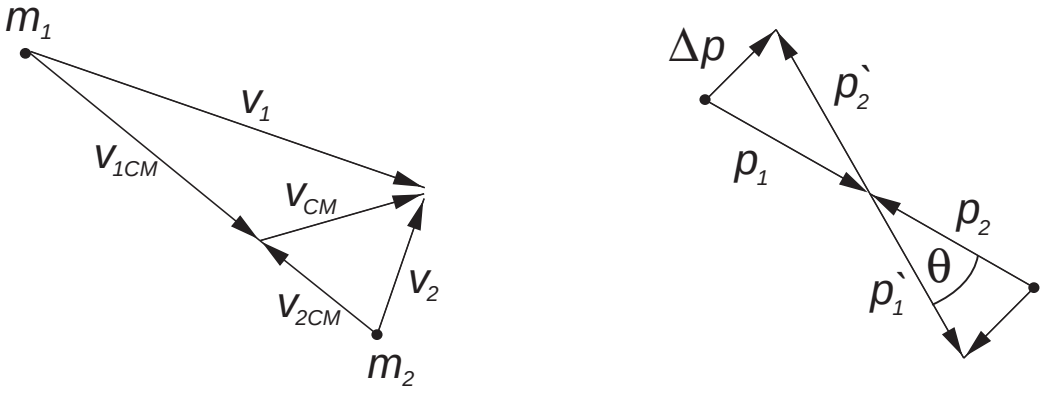

Figure 2: CMS und laboratory system

This momentum transfer is independent of the choice of reference frame, whereas energy and scattering angle depend on this reference frame. In the CM system no energy is transfered. ($E = \frac{p^2}{2m}$). The CM velocity is:

$$\vec{v}_{cm} = \frac{m_1\,\vec{v}_1 + m_2\,\vec{v}_2}{m_1 + m_2} \tag{5}$$

The equations become somewhat more complicated when we transform the coordinates into the laboratory system (LS). We do this by expressing energy and momentum transfer in the LS in terms of the numbers in the CMS (namely the ones above)

$$\begin{aligned}
\triangle\vec{p} &= m_1(\vec{v}_{1CM} + \vec{v}_{CM} - \vec{v}'_{1CM} - \vec{v}_{CM}) = m_1(\vec{v}_{1CM} - \vec{v}'_{1CM}) && (6)\\
\triangle E &= \frac{1}{2}m_1[(\vec{v}_{1CM} + \vec{v}_{CM})^2 - (\vec{v}'_{1CM} + \vec{v}_{CM})^2] \\
&= \frac{1}{2}m_1[\vec{v}^2_{1CM} - \vec{v}'^2_{1CM} + (2\vec{v}_{1CM} - 2\vec{v}'_{1CM})\vec{v}_{CM} + \vec{v}^2_{CM} - \vec{v}^2_{CM}] \\
&= \frac{1}{2}m_1(\vec{v}^2_{1CM} - \vec{v}'^{\,2}_{1CM}) + m_1(\vec{v}_{1CM} - \vec{v}'_{1CM})\vec{v}_{CM} = \triangle p v_{CM} && (7)
\end{aligned}$$

Thus in the LS energy *is* transfered. The smaller the angle between momentum transfer and CM velocity the higher becomes the energy transfer.
Let us consider the case in which the scattered mass m_2 is at rest before the scattering event. We then find: $v_{CM} = \frac{m_1}{m_1+m_2}v_1$. For the transformation between θ, ϑ_1 and ϑ_2 to the following relation applies [1]:

[1] see Landau/Lifschitz Theoretische Physik III Gl.(123,1)

$$\tan(\vartheta_1) = \frac{m_2 \sin(\theta)}{m_1 + m_2 \cos(\theta)}, \qquad \vartheta_2 = \frac{\pi - \theta}{2} \tag{8}$$

When the masses of the scattering partners are identical - as is the case with the nickel nuclei in our experiment - and if a nonrelativistic approximation is valid, this transformation simplifies as follows:

$$\vartheta_1 = \frac{\theta}{2}, \qquad \vartheta_2 = \frac{\pi - \theta}{2} \tag{9}$$

In the laboratory system we find the following relation between scattering angle and energy E_1' of the scattered projectile.

$$E_1 = E_1' + \frac{\vec{p_2'}^{\,2}}{2m_2} \tag{10}$$

$$E_1 = E_1' + \frac{(\vec{p_1} - \vec{p_1'})^2}{2m_2} \tag{11}$$

$$E_1 = E_1' + \frac{1}{2m_2}(\vec{p_1}^{\,2} + \vec{p_1'}^{\,2} - 2 \mid \vec{p_1} \mid \cdot \mid \vec{p_1'} \mid \cdot \cos\vartheta_1) \tag{12}$$

$$E_1 = E_1' + \frac{1}{2m_2}\left[2m_1(E_1 + E_1') - 2\sqrt{4m_1^2\, E_1\, E_1'}\cos\vartheta_1\right] \tag{13}$$

$$E_1 = E_1' + \frac{m_1}{m_2}\left[(E_1 + E_1') - 2\sqrt{E_1\, E_1'}\,\cos\vartheta_1\right] \tag{14}$$

$$\tag{15}$$

$$\boxed{\cos\vartheta_1 = \frac{E_1(1 - \frac{m_2}{m_1}) + E_1'(1 + \frac{m_2}{m_1})}{2\sqrt{E_1\, E_1'}}} \tag{16}$$

In what follows we will try to perform calculations in the CMS and transform the results to the LS afterwards.

1.2 Rutherford scattering

General approaches to describe elastic scattering like partial wave decomposition or the Born-approximation are of quantum-mechanical nature and lack a certain clearness. On the other hand one likes to imagine Coulomb-scattering using a model based on classical trajectories. In fact it is often possible to

describe elastic scattering processes well in a semiclassical or classical approximation. This is particularly true for heavy ion scattering experiments. Using heavy projectiles the De-Broglie-wavelength λ becomes very small and one reaches a regime in which λ is less than the diameter of the scattering potential. As for heavy projectiles the Coulomb barrier is very high though, it is neccessary to perform calculations on the peak of the coulomb-wall with the reduced kinetic energy of the projectile: $E = E_{CM} - V_C$.

For the scattering of 100 MeV ^{12}C projectiles off a carbon target we for example have $\lambda \sim 0.2fm$ After those introductory considerations we have to ask when scattering processes can be approximately described using the picture of classical trajectories. This is the case when the particles are well described by wave-packets during the complete scattering event, i.e. when no significant distortion of the wave packet during the approach to the potential occurs. This in turn is clearly true, when the potential does not change significantly over the range of one wavelength. For the scattering off a point charge one can show that this is the case as long as $2\lambda \ll r_{min}$ (r_{min} = closest approach).

From energy conservation in elastic scattering one can derive that $r_{min} = \frac{2Z_1Z_2e^2}{mv_0^2}$ It is obvious that for the particle energies achievable at the tandem

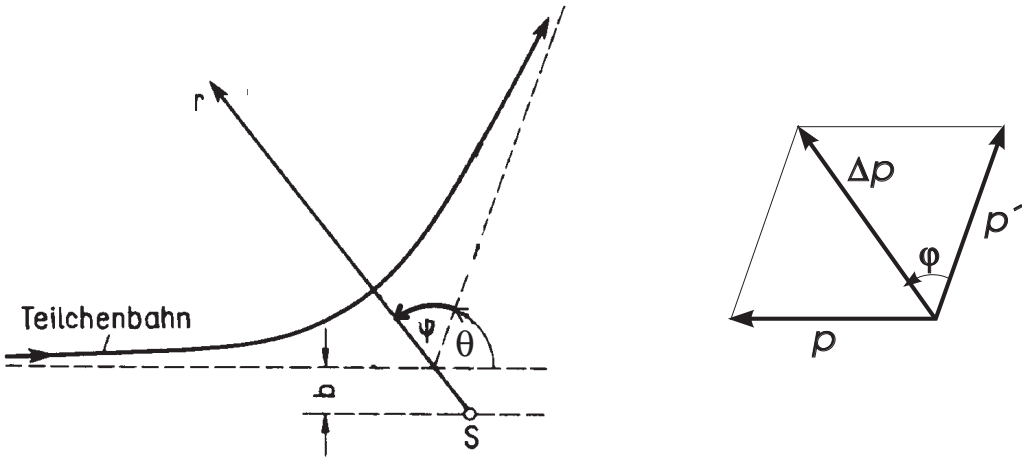

Figure 3: Kinematics of coulomb scattering off the scattering center S.

accelerator (see section 2) a classical treatment of the kinematics is justified to a large extent. A particle of charge Ze in the field of a point charge $Z'e$ experiences the force:

$$F(r) = \frac{Z\,Z'\,e^2}{4\,\pi\,\epsilon_0\,r^2} \tag{17}$$

Introducing the impact parameter b (see Figure 3) its angular momentum is:

$$m\,b\,v\ = I\,\omega = m\,r^2\,\frac{d\,\varphi'}{d\,t} \tag{18}$$

and it experiences a change in angular momentum:

$$\Delta\,p = 2p\,\cos\varphi \ = \ \int F_r\,dt \tag{19}$$

$$\int F_r\,dt \ = \ \int_{-\varphi}^{\varphi} F_r\,\frac{r^2}{b\,v}\,d\,\varphi' \tag{20}$$

$$\int_{-\varphi}^{\varphi} F_r\,\frac{r^2}{b\,v}\,d\,\varphi' \ = \ \int_{-\varphi}^{\varphi} F(r)\,\cos\varphi'\,\frac{r^2}{b\,v}\,d\,\varphi' \tag{21}$$

i.e.

$$2p\,\cos\varphi = \frac{Z\,Z'\,e^2}{4\,\pi\,\epsilon_0\,b\,v}\cdot\int_{-\varphi}^{\varphi}\cos\varphi'\,d\varphi' = \frac{Z\,Z'\,e^2}{4\,\pi\,\epsilon_0\,b\,v}\cdot 2\,\sin\varphi \tag{22}$$

From this however follows:

$$\frac{\sin\varphi}{\cos\varphi} = \frac{4\,\pi\,\epsilon_0\,b\,v}{Z\,Z'\,e^2}\cdot p = \frac{4\,\pi\,\epsilon_0\,b\,2(\frac{1}{2}m\,v^2)}{Z\,Z'\,e^2} \tag{23}$$

Using $\varphi = \frac{\pi}{2} - \frac{\theta}{2}$ this yields:

$$\boxed{\cot\,\frac{\theta}{2} = \frac{8\,\pi\,\epsilon_0\,b\,E_{kin}}{Z\,Z'\,e^2}} \tag{24}$$

In this equation the impact parameter and the scattering angle are related. In physical investigations one is however mostly interested in answering the question: How many particles are scattered towards the detector when a targetelement is irradiated homogeneously? This is described by the differential cross section $\frac{d\,\sigma}{d\,\Omega}$.

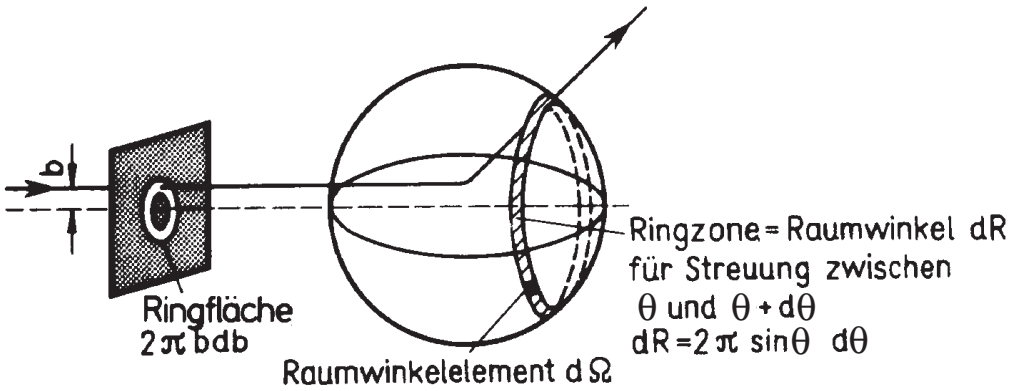

Figure 4: Clarification of the solid angle element $d\Omega$.

$$d\,\sigma = 2\,\pi\,b\,db \tag{25}$$
$$d\,\Omega = 2\,\pi\,\sin\,\theta\,d\theta \tag{26}$$

$$\Longrightarrow \frac{d\,\sigma}{d\,\Omega} = \frac{b}{\sin\,\theta}\frac{db(\theta)}{d\theta} \tag{27}$$

with

$$b(\theta) = \frac{Z\,Z'\,e^2}{8\,\pi\,\epsilon_0\,E_{kin}}\,\cot\,\frac{\theta}{2} \tag{28}$$
$$\tag{29}$$
$$\frac{db(\theta)}{d\theta} = \frac{Z\,Z'\,e^2}{8\,\pi\,\epsilon_0\,E_{kin}}\cdot\frac{-1}{2\,\sin^2\,\frac{\theta}{2}} \tag{30}$$
$$\tag{31}$$
$$\Longrightarrow \qquad \frac{d\,\sigma}{d\,\Omega} = \frac{Z^2\,Z'^2\,e^4}{2\,(8\,\pi\,\epsilon_0\,E_{kin})^2}\cdot\frac{1}{\sin\,\theta}\cdot\frac{\cos\,\frac{\theta}{2}}{\sin^3\,\frac{\theta}{2}} \tag{32}$$

using $\sin\theta = 2\,\sin\frac{\theta}{2}\,\cos\frac{\theta}{2}$ we get for the so called **Rutherford** crosssection:

$$\boxed{\frac{d\,\sigma}{d\,\Omega} = \frac{Z^2\,Z'^2\,e^4}{16\,(4\,\pi\,\epsilon_0\,E_{kin})^2}\cdot\frac{1}{\sin^4\,\frac{\theta}{2}}} \tag{33}$$

1.3 Mott scattering of identical particles

The situation changes when the scattering and the scattered particles are exactly identical, as it is the case for two electrons or in our experiment for two ^{58}Ni - nuclei. Here a special quantum effect manifests itself in the measurement which does not have a classical correspondence.

The Principle of Indistinguishability of Identical Particles.
Here, we encounter a strange exchange-interaction of identical particles, that also has a drastical impact on their scattering [2].

The classical Hamiltonian is in fact symmetric with respect to interchange of identical particles. Nevertheless in quantum-mechanics the symmetry of the wave function with respect to such an interchange has to be taken into account. The states of a system consisting of two identical particles do not change because of the symmetry of the hamiltonian with respect to particle interchange. Let $\psi(\xi_1, \xi_2)$ be the wave function of the system given in the respective coordinates and spin projections, which are combined into ξ_1 and ξ_2. When the coordinates are swapped, the wavefunction can only change by a phase factor α due to the equivalence of the new state:

$$\psi(\xi_1, \xi_2) = e^{i\alpha}\psi(\xi_2, \xi_1) \;\; with \;\; \alpha \in R$$

Performing the swapping a second time, the original wavefunction must be reproduced, i.e. $\psi(\xi_1, \xi_2)e^{2i\alpha} = \psi(\xi_1, \xi_2)$, thus it follows that $e^{2i\alpha} = 1$ and therefore $e^{i\alpha} = \pm 1$. Therefore $\psi(\xi_1, \xi_2) = \pm\psi(\xi_2, \xi_1)$. It is obvious from this, that the wavefunction can only be either symmetric (no change in sign) or antisymmetric (change in sign). It is known, which particle dubletts are described by symmetric wavefunctions - namely boson dubletts and which are described by antisymmetric wavefunctions - namely fermion dubletts. From relativistic quantum mechanics we know that fermions always have a half-integer spin and that bosons always have an integer spin. What are the consequences for the scattering of our ^{58}Ni - nuclei? Our system consisting of beam and target represents precisely a pair of particles, whose wavefunction has to be either symmetric or antisymmetric. Exchanging the particles means that we do not know, whether the beam or the target nucleus has been scattered to the right. This corresponds to a change in sign of their connection-vector. In CMS and spherical coordinates this corresponds to no change in r and a transition from θ to $\pi - \theta$ and from $z = r\cos(\theta)$ to $-z$. This interchange possibility therefore has to be incorporated into the wave function for the assymptotic behaviour of the scattered waves:

[2] This is not to be confused with the spin-orbit interaction which we do not consider here

$$\psi = e^{ikz} + e^{-ikz} + [f(\theta) \pm f(\pi - \theta)]\frac{1}{r}e^{ikr} \tag{34}$$

In the CMS e^{ikz} and e^{-ikz} are two identical matter waves, travelling in opposite directions against one another, which scatter at $z = 0$. The outgoing spherical wave has the same meaning as in Rutherford scattering and takes into account both particles. The expression in brackets preceeding it is also still our scattering amplitude, whose absolute-value square describes the differential cross section. For indistinguishable particles one obtains:

$$\text{for fermions:} \quad \frac{d\sigma_{indi,fermion}}{d\Omega} = |f(\theta) - f(\pi - \theta)|^2 \tag{35}$$

$$\text{for bosons:} \quad \frac{d\sigma_{indi,boson}}{d\Omega} = |f(\theta) + f(\pi - \theta)|^2 \tag{36}$$

Both expressions contain a term $f(\theta)f^*(\pi-\theta)+f^*(\theta)f(\pi-\theta)$. This is an interference term, characteristic for all quantum mechanics. In the classical case, where both particles are identical but distinguishable, the probabilities that the colliding particles are scattered into a solid-angle element $d\Omega$ would simply have to be summed:

$$\frac{d\sigma_{di}}{d\Omega} = |f(\theta)|^2 + |f(\pi - \theta)|^2 \tag{37}$$

The situation is the same as in the double-slit experiment with matter waves and tennis balls. If one carries out the experiment with a statistical multitude of particles, whose spins are not aligned along a field or other direction, one has to average over all possible spin directions. We know that for the projection of its spin s onto the direction of propagation a particle has $(2s+1)$ possibilities. Thus for a two particle system as discussed above $(2 + 1)^2$ possible orientations of the total spin S exist.
From those there are $(2s + 1)$ indistinguishable combinations, in which both particles have the same spin projection ($\Rightarrow \frac{d\sigma_{indi}}{d\Omega}$). The probability that the scattering pair forms one of these combinations is $\frac{2s+1}{(2s+1)^2} = \frac{1}{2s+1}$. The remaining $2s \cdot (2s + 1)$ possibilities are distinguishable, but measured by a detector not sensitive to spin and hence identical ($\Rightarrow \frac{d\sigma_{di}}{d\Omega}$). One obtains a probability of $\frac{2s\cdot(2s+1)}{(2s+1)^2} = \frac{2s}{2s+1}$.
The scattering cross section thus is

$$\frac{d\sigma}{d\Omega} = \left(\frac{1}{2s+1}\right)\frac{d\sigma_{indi}}{d\Omega} + \left(\frac{2s}{2s+1}\right)\frac{d\sigma_{di}}{d\Omega} \tag{38}$$

Inserting (35) and (36) into (38) yields for fermions:

$$\frac{d\sigma}{d\Omega} = |f(\theta)|^2 + |f(\pi-\theta)|^2 - \frac{1}{2s+1}[f(\theta)f^*(\pi-\theta) + f^*(\theta)f(\pi-\theta)] \quad (39)$$

In the same manner we get for bosons:

$$\frac{d\sigma}{d\Omega} = |f(\theta)|^2 + |f(\pi-\theta)|^2 + \frac{1}{2s+1}[f(\theta)f^*(\pi-\theta) + f^*(\theta)f(\pi-\theta)] \quad (40)$$

In our experiment we use $^{58}_{28}$Ni. This is an even-even nucleus and thus has bosonic character with $Z = 28$. Inserting the same scattering amplitude that has yielded the Rutherford scattering formula into that equations, gives the following cross section in the CMS:

$$\frac{d\sigma}{d\Omega} = \frac{Z^4e^4}{4(4\pi\epsilon_0 E_{kin})^2}\left[\frac{1}{sin^4(\frac{\theta}{2})} + \frac{1}{cos^4(\frac{\theta}{2})} + \frac{2}{sin^2(\frac{\theta}{2})cos^2(\frac{\theta}{2})}\cos\left(\frac{Z^2e^2}{4\pi\epsilon_0\hbar v}ln\left(tan^2\frac{\theta}{2}\right)\right)\right] \quad (41)$$

This equation describes the Mott-cross section for identical particles. On a global scale it drops with angle like the Rutherford - cross section, but it is visibly (and measurably) modulated locally by quantum interferences.

1.4 Energy loss in matter

For the identification of charged particles the electromagnetic interaction is used almost exclusively. If a charged particle crosses material, three processes can occur in this interaction: Atoms can be ionized, in special cases Cherenkov-light or transition - radiation is emitted. In the so called absorption-regime only virtual photons are exchanged between the particle and the atoms of the medium, which lead to an excitation or ionization of these atoms and to an energy loss of the particle. The emission of real photons (Cherenkov effect) is possible if the velocity of the particle is larger than the phase velocity of light $c/\sqrt{\varepsilon}$ in the medium. ("Cherenkov-threshold"). If the medium exhibits discontinuities in its index of refraction, there is also the so called "transition radiation".

The differential energy loss dE/dx of an particle with charge z by ionization of atoms in a medium (nuclear charge number Z, atomic mass number A) can approximately be described by the *Bethe-Bloch-formula*:

$$-\frac{dE}{dx} = Kz^2\frac{Z}{A}\frac{1}{\beta^2}\left[\frac{1}{2}ln\frac{2m_ec^2\beta^2\gamma^2T_{max}}{I^2} - \beta^2\right] \quad (42)$$

where $K = 4\pi N_A r_e^2 m_e c^2$, and $r_e = \frac{e^2}{4\pi\varepsilon_0 c^2}$ (classical electron radius).

For a punctual charged particle of mass M, the maximum energy that can be transfered to a free electron in a single collision is T_{max}. It is common practice to approximate T_{max} for low energies by $T_{max} = 2m_e c^2 \beta^2 \gamma^2$. The effective ionization potential I for elements heavier than oxygen is $I = 16 \cdot Z^{0.9}$ eV.

Thus, the energy loss dE/dx depends basically on the charge z but not on the mass M of the ionizing particle. There exists a local ionization minumum with respect to the particle velocity β. For protons this minimum is found at approximately 1 GeV. Below this threshold the energy loss increases again. This is an interesting phenomenon, which has found application in tumor therapy.

The particle energy is adjusted in a way, that most energy is deposited in the depth of the body, where the tumor is located. Therefore, energy deposit in traversed (healthy) tissue can be minimized and mainly cancer affected tissue is destroyed.

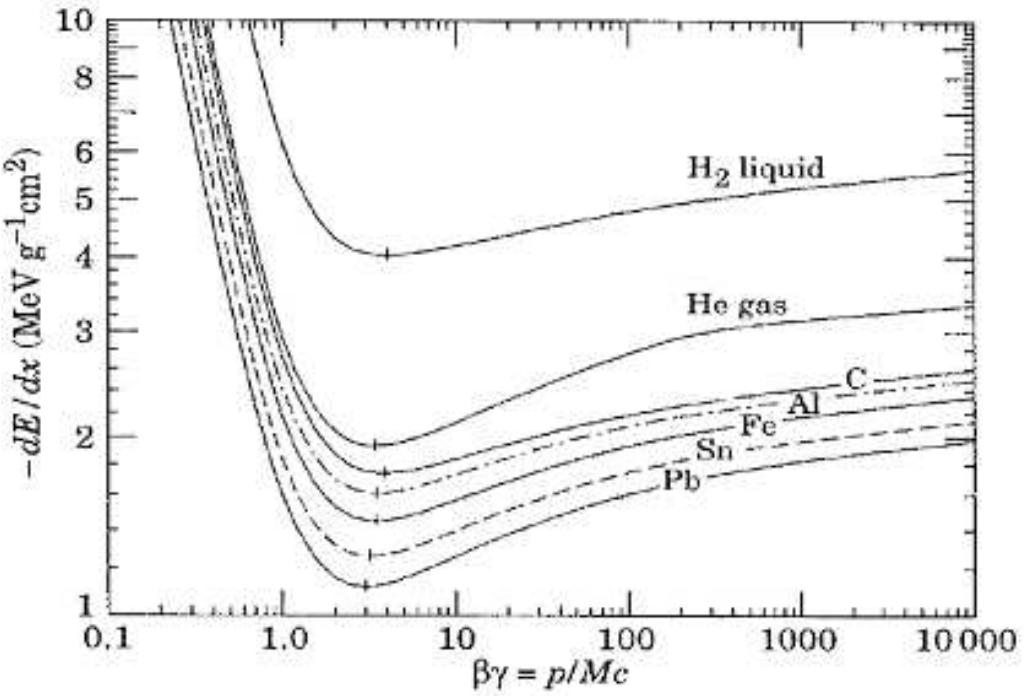

Figure 5: Bethe Bloch formula for different materials

2 The Munich Tandem Accelerator

2.1 Overview

Accelerator devices are required to overcome energy thresholds between atomic nuclei. Such thresholds are e.g. the electrical repulsion of two nuclei or the stripping of all electrons of an ion at the transition through a thin layer of material. In the first case they are used as microscopes for the investigation of atomic nuclei. The accelerator laboratory of the Ludwig Maximilian University Muenchen and the Technical University Muenchen is used by both institutions for the purposes of research and education in the field of nuclear physics and related areas. From an administrative perspective the laboratory is registered as a central institution of the Munich University. The construction of the building started in 1967, since 1971 experiments are conducted. The joint scientific use of the site by reaearch groups of the two universities is coordinated by a research council, whose members are six representatives of the professors, two representatives of the scientific assistants, two representatives of the students and a representative of the nonscientific staff.

The accelerator laboratory is a main educational facility of both Munich universities. Since the start of the experimental operation more than 350 diploma-theses and 160 Ph.D. theses have been completed; The manifold techniques that an experimentalist has to learn and to use, to conduct successful research at an accelerator facility are a good base for a future employment in the area of research and development. As an example analog and digital electronics shall be mentioned, as well as the use of high power computing resources, high-vacuum and high-voltage technology and the use of superconductivity for the realization of static magnetic fields and high-frequency resonators.

2.2 Operating Principle of the Tandem Accelerator

In an accelerator of the elctrostatical type the relation $E = ZeU$ is directly exploited. The main components of an electrostatical accelerator are high-voltage generator, terminal and the vacuum acceleration tube. In the most common type, the Van-de-Graaff-Accelerator, the terminal is constructed as a semi-sphere, which acts as a capacitor with capacity C. To establisch an electrical field, the terminal is charged via an revolving, isolating band. On ground potential positive charge is brought onto this band, which by means of mechanical stripping off is transfered to the terminal. The complete arrangement is placed inside a tank on ground potential and which is filled with isolating gas (e.g. SF_6) to avoid premature breakdown of the voltage.

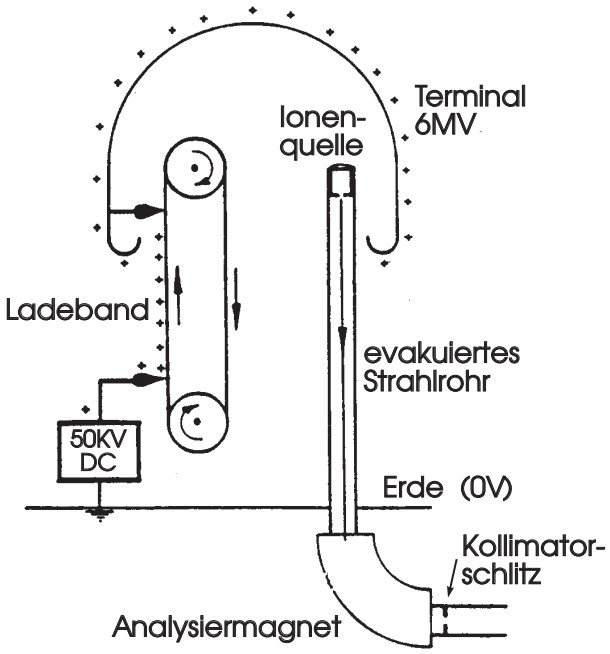

Figure 6: Principal sketch of the Van-de-Graaff-Accelerator

The voltage $U = Q/C$ built up after the charging process can reach up to 15MV. Positive ions, created in an ion source which is on terminal potential, experience the complete potential difference between terminal and tank. Thus protons can be accelerated up to energies of 15MeV.

The main device of the accelerator laboratory is a Tandem-van-de-Graaff-Accelerator with a DC-voltage of up to 15 million volts. The name Tandem stems from the fact that the voltage is used twice by changing the charge of the ions. On ground potential negatively charged ions are created first, which are accelerated in the acceleration tube towards the terminal. There for example a thin foil is located in which the electrons of the ions are partially stripped off, such that the ions are now positively charged. Now the acceleretion voltage is used a second time and the protons can reach up to 30 MeV kinetic energy. Heavy ions can loose several electrons in the strip off event and can respectively reach higher kinetic energies. Van-de-Graaff-accelerators can reliably produce continuous particle beams with currents up to 0.1 mA. They are very important tools for nuclear physics. With them protons, light and heavy ions can be accelerated to energies with which one can study nuclear reactions and perform nuclear spectroscopy in a systematic way.

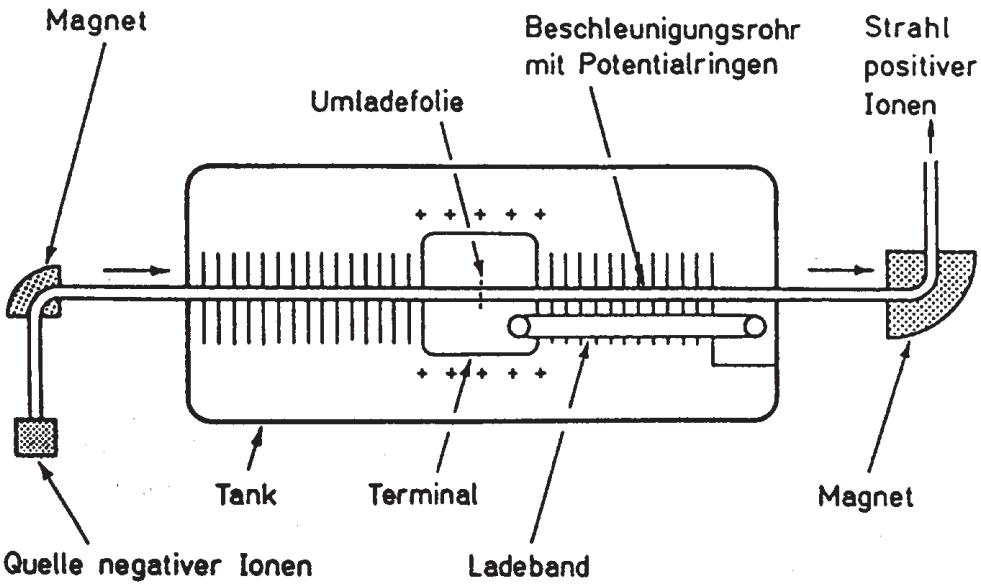

Figure 7: Principal Sketch of a Tandem Accelerator

2.3 Facilities in the Munich accelerator lab

About a dozen measurement sites are available, among them a spectrometer designed for precision measurement of nuclear masses and energies. When the experimental operation started the major science objectives were the analysis of nuclear reactions via measurements of the reaction products and the study of nuclear properties like nuclear structure and mass. It was investigated, whether the nuclei rotate or perform oscillations and how strong they are deformed. In Garching the first successful experimental proof was found that heavy fissioning nuclei in the so called second minimum are strongly deformed ellipsoids, twice as long as thick. About twenty years ago the emphasis was lying on the study of so called "exotic nuclei" with ratio of protons to neutrons which deviates strongly from the one of stable nuclei. Thus for the first time at GSI in Darmstadt and shortly after that at Garching nuclei were produced and identified which decay in their ground state via emission of a proton. Only in those two laboratories were these decays observed. Today's main activities are mass spectrometry with accelerators, material analysis with ion beams, precision measurements of nuclear masses and energies as well as the complete description of nuclear excitations. These measurements allow comparisons with models of nuclei. Due to the activities in the fields of material analysis and accelerator mass-spectroscopy the today's focus of research is in applied physics and interdisciplinary research. Using

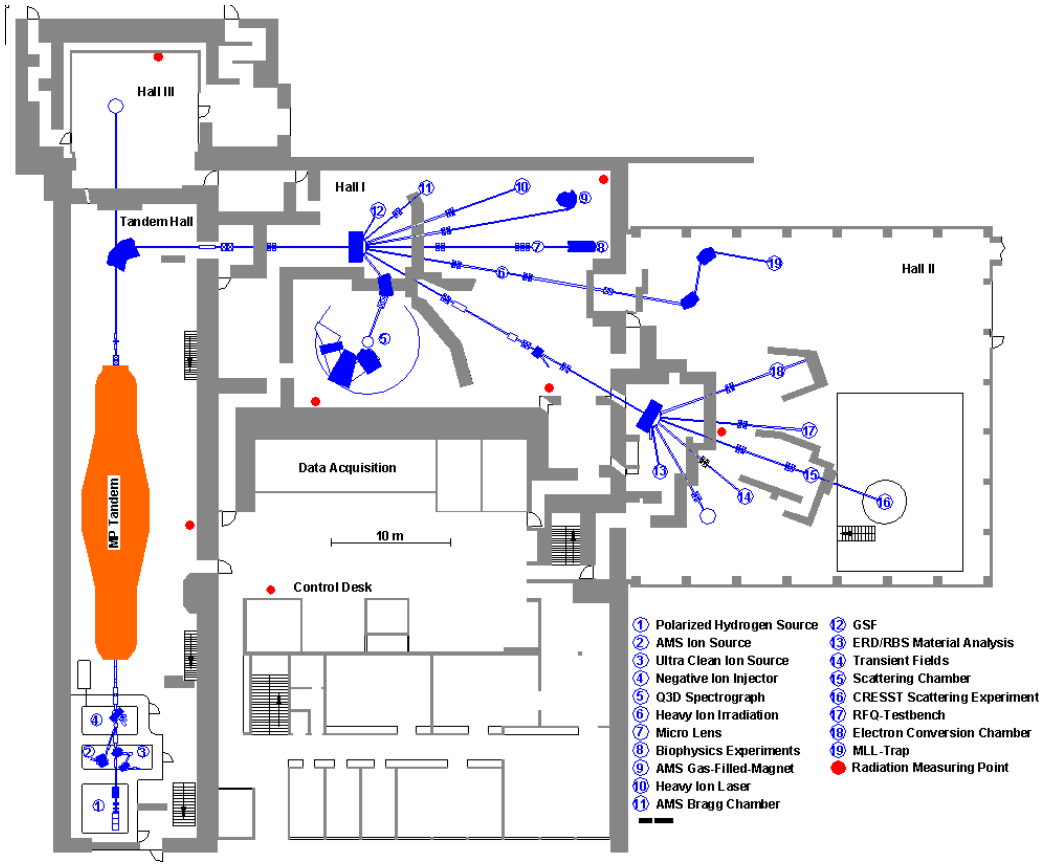

Figure 8: Map of the experimental sites in the Tandem lab

analysis methods from nuclear physics the composition of high-temperature superconductors is investigated for example. Accelerator mass-spectroscopy, developed in first instance at Garching, allows to measure microscopic concentrations of radio-isotopes. With this method a single ^{36}Cl-atom in one billion Cl-atoms can be identified. In this way the age of ground water in a water conducting layer of sand stone after a flow distance of 100 km was determined to be 100 million years. This corresponds to a flow velocity of 1 meter in 10 years. For comparison: The GSF Institut for Hydrologie has estimated that the water used in the munich breweries is about 10 000 to 14 000 years old. Other objects of research are the determination of erosion rates via the measurement of radio-isotopes, which are created by cosmic radiation in the surface of the earth, or test of fundamental physics principles, like the Pauli-principle, which forbids that more than one electron or proton is in the same quantum-mechanical state.

3 Safety Instructions

3.1 Potential hazards in the laboratory

Potential hazards are listed below. During the experiment in the Tandem laboratory, a tutor will be available all the time. If the outcome of your acting is not clear to you, ask your tutor to avoid unnecessary hazards.

- High Voltage: The detectors are biased with a voltage up to 50V. Only adequate HV-cables are allowed to be used.
- No eating and drinking is allowed in the laboratory and machine shops.
- Sturdy shoes are mandatory in the laboratory and in machine shops.
- Working with radioactivity requires special precaution and knowledge of the user. See the next Subsection for details.

3.2 Basics of radiation safety

According to §55 StrlSchV (Radiation safety regulation) dated 20.07.01 the acceptable radiation dose for people exposed to radiation occupationally is: 20 mSv/year.
For an unborn child, which is exposed to radiation because of the employment of the mother, the overall dose is 1mSv.

Unit: Sievert 1Sv = 100rem = 1 J/kg

According to medical studies such doses do not cause somatic or chronic damage. Because of possible genetic damage we want to avoid reaching those doses! A genetic damage can be done even by the smallest dose and is not reparable, because during cell division the same (damaged) cell is reproduced every time. Such a mutation is normally recessive in nature - which means that it is not detectable in the first generation of offspring. However a existing damage in the genomic heritage will always be bequeathed.

Thus we make a strict point: We take measures to absorb as low a radiation dose as possible!

- Entering experimental halls:
  To keep the absorbed dose as low as possible, we observe the following rule:

more than 1 mSv/h	:	Do not enter!.
0.1-1 mSv/h	:	just a few minutes, (to do just a few things).
20-100 μ Sv/h	:	no longer than half an hour.
5-20 μ Sv/h	:	no longer than two hours.
Less than 5 μ Sv/h	:	no limitation.

If we comply with this rule we maximally accept 2mSv/year, which is comparable to the radiation dose absorbed from natural sources. This should be an acceptable dose. One monitor in the control room shows the radiation level for the whole controlled area.

- Radiation measurement and warning system:

  - Yellow blinking light: Attention - beam on! Take care! Ask operator before performing any action!

  - Blue blinking glight: Leave hall immediately! (and siren) Acute danger!

- **Eating, drinking and smoking is forbidden in the complete control area!**

- Please take always a dosimeter with you, when you enter the control area. This is the only possibility to measure your personalized dosis and to detect possible damage early! The stick-dosimeters have to be read out every working day (starting from 0.2 mSv (=20 mrem) one has to report the radiation safety officer).

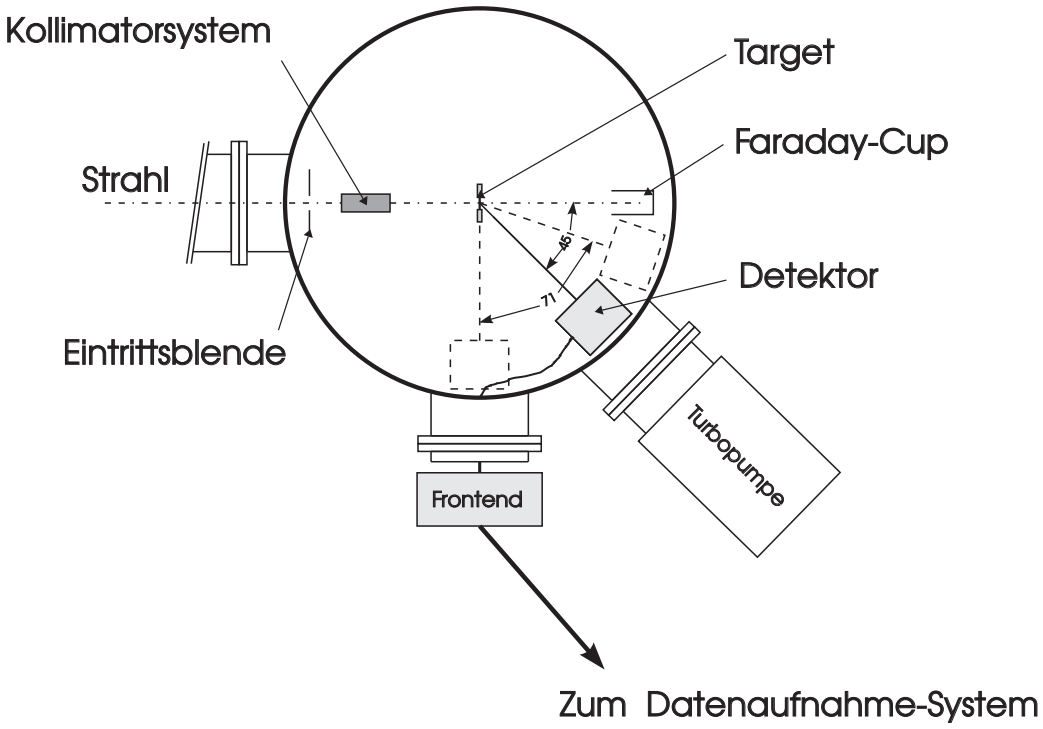

Figure 9: Experiment setup.

4 Experiment setup and execution

4.1 Assembly

The experiment is set up in target hall II of the accelerator lab in the heavy-ion scattering chamber marked with reference numeral 15 on the site map (figure 8). The beam is lead to this scattering chamber continuously through vacuum beam pipes, which requires a huge number of beam deflection devices in order to focus the beam onto the target in the center of the scattering chamber. Beam guidance is controlled in the control room of the accelerator by the responsible operators, which "thread" the beam to the respective experiment. Figure 9 shows the principle arrangement of the scattering chamber (hall II $-10°$). The particle beam enters the chamber from the left and is guided upon the target by an aperture and a collimator system. The target is brought into the target chamber through the chamber cover in a vacuum tight manner. The particles passing the target undeflected are collected in a so called Faraday-Cup, which also serves for monitoring the beam current. On the bottom of the chamber a vacuum tight rotary motion feedthrough is

located, which allows the experimentalist to change the angular position of the detector system from outside, without having to open and thus ventilate the scattering chamber. Parts of the analog readout electronics are attached directly in respectively at the chamber to avoid noise and distortions of the delicate signals on long signal transmission lines. All electrical connections also must be manufactured vacuum tight. Apart from the experimental setup vacuum pumps and vacuum measurement devices are mounted at the chamber.

4.2 Particle detectors

Semiconductor counters work like solid-state ionization chambers. A charged particle – in case of photon detection a photo-electron – creates electron-hole pairs on its way through the crystal. The crystal is arranged between two electrodes, which create an electrical field. During the ionization in semiconductors the electrons acquire activation energies of up to 20 keV by scattering events of the charged particle. They are lifted from the valence band to the conduction band and leave a hole in the valence band. In secondary processes electrons then loose their energy step by step, by creation of further electron-hole pairs (excitons) and by excitation of lattice oscillations (phonons). What remains is a plasma hose with a high concentration of electrons and holes (10^{15} – $10^{17}/\mathrm{cm}^3$) along the trajectory of the primary charged particle. If it is possible to collect the electrons on the anode, before they recombine with holes, the primary particle can be detected and the deposited energy can be measured. To create an electron- hole pair in Silicon (Germanium) an energy of only 3.6 eV (2.8 eV) is required, whereas the ionization energy is between 20 and 40 eV is gases. In scintillation counters even 400 to 1000 eV are required, to excite a photoelectron in the photocathode via the scintillation process. As a material for such solid state counters high purity semiconductor-mono-crystals made of Silicon or Germanium are used. Those semiconductors are operated as diodes in reverse bias mode to effect high electrical fields in the crystal for the collection of electrons. Three types of semiconductor detectors have found practical application: Diodes with p-n transition, with surface depletion layer and with p-i-n structure.

A p-n transition in semiconductors is the boundary layer between a zone doped with p-impurities (electron-acceptors) with hole-conduction and a zone doped with n-impurities (electron-donators) with electron-conduction. An asymmetric p-n-transition consists of weakly doped material, which has been provided from one surface with a thin but strongly doped n-layer.

On the boundary between the different dopings a charge double-layer develops. The resulting potential difference results in a charge carrier cur-

rent, which effects a depletion of the boundary layer of free charge carriers. ("Depletion zone", "barrier layer"). This n-p-layer acts like a diode. In the band-model of the semiconductor potential difference and the deformation of valence- and conduction band arises from the fact that in the n-doped semiconductor the fermi-level is higher than in the p-doped one. As the fermi niveau of the connected p- and n-layer must be equal, the bands deform. If one applies an outer voltage in reverse-bias direction – i.e. a negative voltage on the p-layer – the depth of the depletion layer increases. As the regions of the crystal adjacent to the barrier layer have higher conductivity than this layer, the major part of the voltage drops over the barrier layer. Thus the field strength is strongest there and enough to extract the major part of the free electrons from the barrier layer, before those can recombine. In a simplified 1-dimensional model the thickness of the barrier layer can be computed. The Poisson equation for the potential U(x) for a charge density ρ is:

$$\frac{d^2U(x)}{dx^2} = \frac{\rho(x)}{\varepsilon_0\varepsilon} \tag{43}$$

with $E_x = \frac{dU}{dx}$

$$\frac{dE_x(x)}{dx} = \frac{\rho(x)}{\varepsilon_0\varepsilon} \tag{44}$$

. Let N_D and N_A be the densities of donor- and acceptor-impurities respectively. The asymmetric doping results in the charge distribution

$$\rho(x) = \begin{cases} eN_D & \text{for } -a < x \leq 0 \\ -eN_A & \text{for } 0 < x \leq b \end{cases}$$

where $N_D \gg N_A$ and $a < b$. The boundary conditions for the electrical field are $E_x(-a) = 0 = E_x(b)$. The first integration of equation (43) thus yields:

$$\frac{dU}{dx} = \begin{cases} -\frac{eN_D}{\varepsilon_0\varepsilon}(x+a) & \text{for } -a < x \leq 0 \\ \\ +\frac{eN_A}{\varepsilon_0\varepsilon}(x+b) & \text{for } 0 < x \leq b \end{cases}$$

For the potential the following boundary conditions apply: $U(-a) = 0$ and $U(b) = -U_0$ The second integration then yields:

$$U(x) = \begin{cases} -\frac{eN_D}{2\varepsilon_0\varepsilon}(x+a)^2 & \text{for } -a < x \leq 0 \\ \\ +\frac{eN_A}{2\varepsilon_0\varepsilon}(x+b)^2 - U_0 & \text{for } 0 < x \leq b \end{cases}$$

The solution for $U(x)$ must be continuous at $x = 0$ and the charges at the double layer compensate one another ($N_D a = N_A b$), such that:

$$b(a+b) = \frac{2\varepsilon_0 \varepsilon U_0}{eN_A} \tag{45}$$

. Because of $N_D \gg N_A$ the thickness of the p-doped layer b is much bigger than a, and thus it follows that $d = a + b \approx b$, which in turn gives:

$$d = \sqrt{\frac{2\varepsilon_0 \varepsilon U_0}{eN_A}} \tag{46}$$

As the impurity concentration is inversely proportional to the specific resistance ρ_p of the base material (pSi) multiplied with the mobility μ of the charge carriers – i.e. $1/(eN_A) = \rho_p \mu$, another formulation of relation (46) can be written:

$$d \approx \sqrt{2\varepsilon_0 \varepsilon U_0 \rho_p \mu} \tag{47}$$

The highest field strength exist at $x = 0$;

$$E_x(0) = \sqrt{\frac{2eN_A U_0}{\varepsilon_0 \varepsilon}} = \frac{2U_0}{d} \tag{48}$$

For $d = 100\,\mu m$ und $U_0 = 200$ V we find: $E_x(0) = 4 \cdot 10^6$ V/m. This is sufficient to separate a large part of the electrons and holes set free via ionization processes in the silicon and to suck the electrons to the anode. The collection times t_c can be estimated: For a counter thickness s of 300μm an average field of $2 \cdot 10^5$ V/m and an electron mobility of $\mu = 2 \cdot 10^4\, cm^2/Vs$ we find:

$$t_c = \frac{s}{\mu E} \sim 1ns \tag{49}$$

A barrier layer can also be created via metal-semiconductor contact. Commen are counters in which on an n-doped silicon-mono-crystal a gold layer is deposited by a vapor deposition process. Counter areas of up to 10 cm^2 at a barrier layer thickness of 50 μm or areas of 1 cm^2 with a thickness of up to 2mm are feasible. Inserting numbers for the constants in equation (47), we find for the mentioned detector type the following relation for the dependence of the barrier layer thickness on the applied reverse-bias voltage U and on the specific resistance ρ of a silicon-mono-crystal:

$$d = 0.309\sqrt{U \cdot \rho_p} \quad \text{for p-doped Si [} d \text{ in } \mu m,\ U \text{ in } V,\ \rho \text{ in } \Omega cm] \tag{50}$$

$$d = 0.505\sqrt{U \cdot \rho_n} \quad \text{for n-doped Si [} d \text{ in } \mu m,\ U \text{ in } V,\ \rho \text{ in } \Omega cm] \tag{51}$$

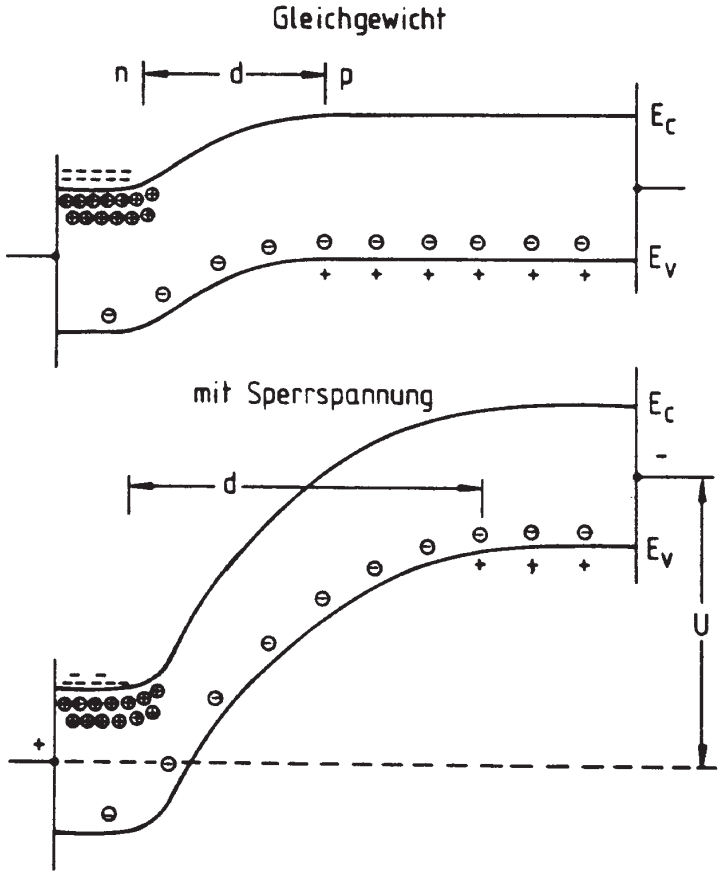

Figure 10: Band structure of an asymetrical p-n transition; d: thickness of depletion layer, E_c: lower boundary of conduction band, E_v: upper boundary of valence band, U: reverse-bias voltage.

Particularly thick depletion layers can be achieved, by creating a layer in which the impurities are compensated completely by drift of ions of opposite electron affinity between a n- and a p-doped zone in the semiconductor crystal. As a base material one choses e.g. Borium doped p-silicon with a specific resitance of 100 to 1000 Ωcm. Then Lithium ions (donators) are allowed to diffuse into the crystal from one of the surfaces. In this way a n-layer is created on this surface and in an intermediate area the diffusion process can be controlled such that the number of Lithium ions becomes just equal the number of Borium ions, whereby the specific resistance in this depletion layer rises to $3 \cdot 10^5 \Omega cm$. This is the specific resistance value for self-conductivity of silicon without impurities, because if which the layer is called i-layer ("in-

trinsic conductivity"). At an applied outer reverse-bias voltage the complete depletion layer becomes the barrier layer. In this way barrier layers with a thickness of up to 5 mm can be manufactured. Considering the range diagram, we see that with such counters α particles with energies of up to 200 MeV and electrons with energies up to 2 MeV can be absorbed in this barrier-layer. This means that the accumulated charge in this energy range is proportional to the energy E_0 of the incident particle. In this range the energy resolution of the semiconductor detector is better as the resolution of other detectors. The number n of free electron-hole pairs is $n = E_0/W_i$ with $W_i = 3.6$ eV (2.8 eV) for Si(Ge). The statistical fluctuation of this number is $\sqrt{n}$. Here it is even reduced by the so called Fano-effect (energy loss in a collision is not purely statistical), such that $\sigma_n = \sqrt{nF}$ with the Fano-factor $F \approx 0.09$ to 0.14 in Si and $F \approx 0.06$ to 0.12 in Ge at a Temperature of 77 K. The relative energy resolution is thus:

$$\frac{\sigma(E)}{E_0} = \sqrt{\frac{FW_i}{E_0}} \tag{52}$$

For a Germanium detector one expects thus as the best possible energy resolution for a photon with energy $E_0 = 8$ MeV: $\sigma(E)/E_0 = 1.5 \cdot 10^{-4}$ and for a photon with $E_0 = 122$ keV:$\sigma(E)/E_0 = 1.2 \cdot 10^{-3}$. Indeed for those two energies resolutions of $5.4 \cdot 10^{-4}$ and $7.1 \cdot 10^{-3}$ respectively have been measured, which do not quite reach the principal limit.

4.3 Analog und Digital Signal Processing

The signals created in the detector have to be electronically processed further. To this aim an elaborate system of several electronics components is used. Those are partially commercially available in a standardized fashion or have been manufactured in the institute's electronics shop. In this way also basic electronics skills are taught in a clear way in this experiment.

First the signals of both sides of the detector are separated and input to analog amplifiers, which integrate the created charge, amplify it and transform it to a voltage signal. This signal is handed to a pulse shaper and main amplifier as well as parallel to that to a discriminator, which delivers a square pulse and activates the trigger logic if the signal surpasses a certain threshold. In this way an AD-converter is informed when a signal will arrive, which is to be registered. The AD-converter then sends the binary data to a measurement computer, which records the data. Here C++ programs are installed which post-process and visualize the data. From a physical point of view we work with 4 channels (2 sides of 2 detectors). The charge which

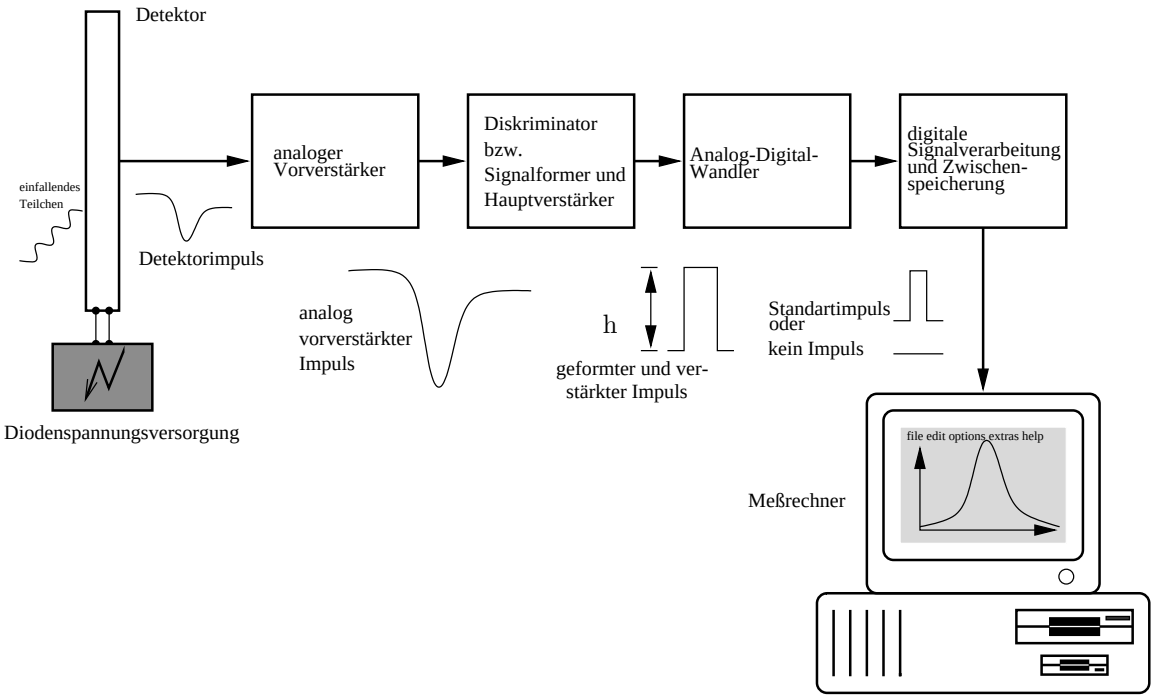

Figure 11: Schematic setup of the data aquisition of the experiment

is created when a particle hits the detector - a so called "Position Sensitive Diode - PSD" is split on the surface of the detector via a resistance layer and is read out proportionally on both ends of the detector. The position information is calculated from the difference of the two signal pulses, the total energy from their sum.

4.4 Experimental procedure

Your task in this experiment is to measure the differential cross section for scattering of a ^{58}Ni ion on a ^{58}Ni target. In your written report the measured values are to be compared with the theoretical prediction and any deviations are to be justified using physical arguments.

In the previous chapters of this manual you have learned about the experimental setup as well as the method of measurement.

The experimental procedure can be structured into three sections:

1. In the morning of the first day radiation safety, progress of the experiment and physical understanding are discussed in a seminar. You will have to prepare a topic that will be assigned before the lab course.

Examples

(a) Kinematical considerations in scattering processes

(b) Energy loss of high energy particles in matter

(c) Aspects of Mott-scattering

(d) ....

In addition to that, there will be a 1 hour guided tour through the Tandem Accelerator lab. In the afternoon, different groups start to set up the experiment in shifts.

2. On the second day, the setup of the experiment is continued in shifts.

3. On the last day the experiment itself is conducted and data is taken.

The data analysis will be part of the written report.

During the complete setup and data aquisition a protocol has to be taken, of which you will receive a copy. It is essential that in this protocol all steps of the experiment and all parameters as well as all theoretical considerations and sketches are recorded properly and uniquely. Whatever you forget here can eventually endanger the success of the complete effort, as later on some particular information (cable ordering, amplifier setting) may not be available any longer! The experiment itself will progress approximately like this:

- After you have become aquainted to the apparatus, the various components for the measurement in the vacuum scattering chamber will be assembled first.
- The electronic signal processing and data acquisition devices are cabled and tested via test pulses.
- Now detectors and data acquisition can be adjusted with a radioactive α -source. In this way an experiment-like state is already realized with the only exception that the particles do not come from the target.
- At last the target is inserted into the scattering chamber, which is then evacuated up to high vacuum level 10^{-6} mbar.
- After this the operator on shift will ramp up the tandem accelerator and the beam is threaded through many meters of beam pipe up to the experiment. This is achieved by variation of magnet currents of many dipols and quadrupols in interaction various beam sensors. With

those sensors the beam current can be measured and you can check the detector signals with the help of an oscilloscope.

- Now the real measurement starts: The detectors have a fixed position with respect to the target and extend over a finite range in angle with respect to the interaction point. Measuring count rates and deposited energies at different angular positions we will be able to reconstruct the Mott scattering cross section from the data.